Journal of Sound and Vibration (1999) **226**(5), 955–983
Article No. jsvi.1999.2306, available online at http://www.idealibrary.com on IDEAL®

GEOMETRICAL NON-LINEAR, STEADY STATE, FORCED, PERIODIC VIBRATION OF PLATES, PART I: MODEL AND CONVERGENCE STUDIES

P. RIBEIRO† AND M. PETYT

Institute of Sound and Vibration Research, University of Southampton, Southampton SO17 1BJ, England

(*Received* 28 *August* 1998, *and in final form* 22 *March* 1999)

A model for the steady state, geometrically non-linear, periodic vibration of thin rectangular plates under harmonic external excitation is presented. The equations of motion in the time domain are derived by applying the principle of virtual work and the hierarchical finite element method (HFEM). These equations are transformed into the frequency domain by the harmonic balance method (HBM) and are solved by a continuation method. The convergence properties of the model are discussed by applying it to isotropic and to composite laminated plates.

1. INTRODUCTION

When thin plates are subjected to large dynamic excitation levels, they can undergo large-amplitude, geometrical non-linear vibrations. This occurs typically with aircraft skin-panels, which are subjected to high levels of acoustic pressure and of aerodynamic forces.

Geometrical non-linear vibrations are modelled by non-linear equations, the solution of which frequently can be only obtained by iterative methods. In each iteration, the non-linear matrices are reformulated and, therefore, the time required to solve the equations of motion increases significantly with the number of degrees of freedom (d.o.f.) of the model. Consequently, various approximations have been followed. Often, the solution is considered to be a function of a very limited number of linear—thus constant—modes, simplifying the response to a function of one or two variables [1–9].‡ In references, [10, 11], a modal reduction method was used to transform the system of equations of motion in physical co-ordinates into normal co-ordinates, thus reducing the size of the matrices. The normal co-ordinates are the linear modes, which are determined by using a finite element method (FEM) model.

†Present address: DEMEGI, Faculdade de Engenharia, Universidade do Porto, Rua dos Bragas, 4099 Porto Codex, Portugal.

‡In reference [4] solutions with more than two unknowns are also presented.

0022-460X/99/400955 + 29 $30.00/0

It is well known that, due to the effect of the membrane forces, the plate's mode shapes generally vary with the amplitude of vibration displacement [12–16]. The FEM leads to an accurate spatial model and allows one to describe the variation of the mode shape of the plate with the amplitude of vibration displacement. In references [17, 18], a triangular element and the *h*-version of the FEM were used to analyze free and forced vibration of an undamped simply supported plate. The equations of motion were solved by incrementing selectively the fastest varying characteristic amplitude or the frequency. Two harmonics were used and loops due to 1 : 3 internal resonances were found. In references [19, 20], the hierarchical, *p*-version of the finite element method was applied to analyze the consequences of internal resonances on the multi-frequency free vibration of plates. It was shown that internal resonances result in an important change of the plates mode shape not only with the amplitude of vibration displacement but also during the period of vibration. Most of the other applications of the finite element method (FEM) to the study of geometrical non-linear vibration of plates, are restricted to harmonic vibrations [21–28].

In the *p*-version of the FEM, the accuracy of the approximation is improved by increasing the number of shape functions over the elements, as opposed to the *h*-version in which the mesh is refined. If the set of functions corresponding to an approximation of lower order p, constitutes a subset of the set of functions corresponding to the approximation of order $p + 1$, then the *p*-version of the FEM is called the "hierarchical finite element method" (HFEM). The HFEM usually requires a fewer degrees of freedom than the *h*-version of the FEM [14–16, 19, 20, 27–29].

The motion of plates excited by harmonic forces and vibrating with displacement amplitudes of the order of their thickness is generally periodic [29] and, consequently, can be analyzed by the harmonic balance method (HBM) [30–32].

In non-linear vibrations turning and bifurcation points may exist, leading to regions with multiple solutions. Continuation methods [33] are able to pass turning points to discover bifurcation points and, in most cases, to follow secondary branches. Continuation methods are computationally heavier than other simpler methods, making it even more important to have an accurate model with a reduced number of d.o.f.

In this paper, the HFEM method is used to construct the geometrical non-linear spatial model of thin, rectangular, isotropic and composite laminated plates. The harmonic balance method is applied to transfer the equations of motion into the frequency domain, which are solved by a continuation method. The response of the plates to external harmonic excitations is analyzed, concentrating on the convergence of the solution with the number of harmonics and with the number of shape functions. Fully clamped boundaries are considered because they are adequate to model many real panel-type situations, such as aircraft wing panels [14]. However, the methods presented can be applied to plates with any boundary conditions. In a companion paper [34], the stability of the solutions and the effects of internal resonances on the steady state forced vibration of plates are investigated.

2. EQUATIONS OF MOTION

2.1. HIERARCHICAL FINITE ELEMENT MODEL

The HFEM model presented here was developed in reference [14] and has been applied to the study of geometrical non-linear free [14–16, 19, 20] and forced [19, 20] harmonic vibration of plates, and to the free multi-harmonic vibration of plates [27, 28]. For each element, the middle-plane displacements u_0, v_0 and w_0 (see Figure 1) are expressed in the form

$$\begin{Bmatrix} u_0 \\ v_0 \\ w_0 \end{Bmatrix} = [N] \begin{Bmatrix} q_p \\ q_w \end{Bmatrix}, \quad [N] = \begin{bmatrix} \lfloor N^u \rfloor & 0 & 0 \\ 0 & \lfloor N^u \rfloor & 0 \\ 0 & 0 & \lfloor N^w \rfloor \end{bmatrix}, \tag{1, 2}$$

$$\lfloor N^u \rfloor = \lfloor g_1(\xi)g_1(\eta) \;\; g_1(\xi)g_2(\eta) \cdots g_{p_i}(\xi)g_{p_i}(\eta) \rfloor, \tag{3}$$

$$\lfloor N^u \rfloor = \lfloor f_1(\xi)f_1(\eta) \;\; f_1(\xi)f_2(\eta) \cdots f_{p_o}(\xi)f_{p_o}(\eta) \rfloor, \tag{4}$$

where p_i and p_o are the number of in-plane and out-of-plane shape functions used in the model; $\{g\}$ and $\{f\}$ are the vectors of in- and out-of-plane shape functions; $\{q_p\}$ and $\{q_w\}$ are the generalized in- and out-of-plane displacements and $[N]$ the matrix of shape functions. The shape functions used are the Rodrigues' form of Legendre polynomials [14, 19, 29].

For smooth solutions, the introduction of higher order shape functions gives a greater accuracy per number of d.o.f. than a refinement of the mesh [35]. Therefore, the whole plate is modelled with one element only and the relation between the local and global co-ordinates is

$$\xi = 2x/a, \qquad \eta = 2y/b. \tag{5}$$

The shape functions used satisfy fully clamped boundary conditions. To analyze plates with different boundary conditions or if more than one element is necessary, other shape functions—for example third order polynomials as used in the *h*-version of the FEM—are added to the model.

Only thin plates are analyzed, and thus the thin plate theory, in which the transverse shear is neglected, allows accurate prediction of the displacements

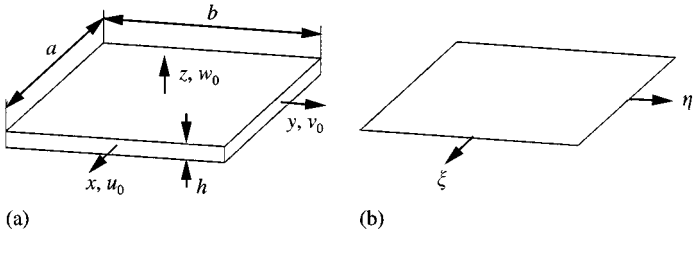

Figure 1. (a) Rectangular plate: x, y, and z—global co-ordinate system; u_0, v_0 and w_0—middle plane displacements; a, b and h—plate dimensions. (b) ξ, η—local co-ordinate system.

of the plate and will be used. In thin plates, rotatory inertia can also be neglected [4].

The geometrical non-linearity is expressed by the non-linear strain–displacement relationships of von Kármán, which are given by

$$\begin{Bmatrix} \varepsilon_x \\ \varepsilon_y \\ \gamma_{xy} \end{Bmatrix} = \begin{bmatrix} 1 & 0 & 0 & z & 0 & 0 \\ 0 & 1 & 0 & 0 & z & 0 \\ 0 & 0 & 1 & 0 & 0 & z \end{bmatrix} \{\varepsilon\} = [[I] \;\; z[I]]\{\varepsilon\}, \tag{6}$$

where

$$\{\varepsilon\} = \begin{Bmatrix} \varepsilon_o^p \\ \varepsilon_o^b \end{Bmatrix} + \begin{Bmatrix} \varepsilon_L^p \\ 0 \end{Bmatrix}. \tag{7}$$

$\{\varepsilon_o^p\}$ and $\{\varepsilon_o^p\}$ are the linear membrane and bending strains; and $\{\varepsilon_L^p\}$ is the geometrically non-linear membrane strain. They are defined as

$$\{\varepsilon_o^p\} = \begin{Bmatrix} u_{,x} \\ v_{,y} \\ u_{,y} + v_{,x} \end{Bmatrix}, \qquad \{\varepsilon_o^b\} = \begin{Bmatrix} -w_{,xx} \\ -w_{,yy} \\ -2w_{,xy} \end{Bmatrix}, \qquad \{\varepsilon_L^p\} = \begin{Bmatrix} (w_{,x})^2/2 \\ (w_{,y})^2/2 \\ -w_{,x}w_{,y} \end{Bmatrix}, \tag{8}$$

where subscript ,x (,y) denotes differentiation with respect to x (y).

In this paper, the external forces are applied only in the transverse direction. The equations of motion are derived by equating the sum of virtual work of the inertia forces, of the elastic restoring forces and of the external forces to zero. Only isotropic and symmetric laminated plates will be analyzed; consequently, there is no coupling between in-plane stretching and transverse bending, i.e., the matrix usually represented by $[B]$ is equal to zero, and so

$$\int_\Omega (\{\delta\varepsilon_o^p\}^{\mathrm{T}} + \{\delta\varepsilon_L^p\}^{\mathrm{T}})[A](\{\varepsilon_o^p\} + \{\varepsilon_L^p\})\,\mathrm{d}\Omega + \int_\Omega \{\delta\varepsilon_o^b\}^{\mathrm{T}}[D]\{\varepsilon_o^b\}\,\mathrm{d}\Omega$$

$$+ \int_\Omega \rho h(\delta u_0\ddot{u}_0 + \delta v_0\ddot{v}_0 + \delta w_0\ddot{w}_0)\,\mathrm{d}\Omega = \lfloor \delta u \;\; \delta v \;\; \delta w \rfloor \int_\Omega [N]^{\mathrm{T}} \begin{Bmatrix} 0 \\ 0 \\ \bar{P}_d(x, y, t) \end{Bmatrix}, \tag{9}$$

where ρ denotes the mass density; $\bar{P}_d(x, y, t)$ is the distributed applied force (N/m^2) and Ω is the area of the plate. $[A]$ and $[D]$ are the membrane and flexural rigidity matrices given by

$$(A_{ij}, D_{ij}) = \sum_{k=1}^{NL} \int_{z_{k-1}}^{z_k} (1, z^2) C_{ij}^{(k)}\,\mathrm{d}z, \quad i, j = 1, 2 \text{ and } 6. \tag{10}$$

Here $C_{ij}^{(k)}$ are the reduced stiffnesses of the kth layer, which can be obtained from E_L, E_T, the major and minor Young's moduli, the Poisson ratios v_{LT} and v_{TL} and the shear modulus G_{LT} [4]. L and T denote the principal directions of the orthotropic plate layer. For isotropic plates, matrices $[A]$ and $[D]$ are simplified to

$$[A] = \frac{Eh}{(1-v^2)} \begin{bmatrix} 1 & v & 0 \\ v & 1 & 0 \\ 0 & 0 & \frac{1}{2}(1-v) \end{bmatrix} \quad \text{and} \quad [D] = \frac{h^2}{12}[A]. \tag{11, 12}$$

Substituting equations (8) into equation (9) and allowing the virtual generalized displacements to be arbitrary gives

$$\begin{bmatrix} M_p & 0 \\ 0 & M_b \end{bmatrix} \begin{Bmatrix} \ddot{q}_p \\ \ddot{q}_w \end{Bmatrix} + \left(\begin{bmatrix} K_{1p} & 0 \\ 0 & K_{1b} \end{bmatrix} + \begin{bmatrix} 0 & K_2 \\ 0 & 0 \end{bmatrix} + \begin{bmatrix} 0 & 0 \\ K_3 & 0 \end{bmatrix} + \begin{bmatrix} 0 & 0 \\ 0 & K_4 \end{bmatrix} \right) \begin{Bmatrix} q_p \\ q_w \end{Bmatrix} = \begin{Bmatrix} 0 \\ \bar{P} \end{Bmatrix}. \tag{13}$$

$[M_p]$ and $[M_b]$ are the in-plane and bending inertia matrices; $[K_{1p}$ and $[K_{1b}]$ the in-plane and bending linear stiffness matrices; $[K_2]$, $[K_3]$ and $[K_4]$ the non-linear stiffness matrices and $\{\bar{P}\}$ is the vector of generalized external forces. $[K_2]$ and $[K_3]$ depend linearly on $\{q_w\}$ and $[K_4]$ depends quadratically on $\{q_w\}$. All submatrices in equation (13) are symmetric except $[K_2]$ and $[K_3]$, which are related by $[K_3] = 2[K_2]^{\mathrm{T}}$ [14].

Upon neglecting the middle-plane in-plane inertia, and thus eliminating the in-plane generalized displacements, and introducing mass proportional hysteretic damping the following equations of motion are obtained:

$$[M_b]\{\ddot{q}_w\} + (\beta/\omega)[M_b]\{\dot{q}_w\} + [K_{1b}]\{q_w\} + [Knl]\{q_w\} = \{\bar{P}\}. \tag{14}$$

Here $[Knl] = [K_4] - 2[K_2]^{\mathrm{T}}[K_{1p}]^{-1}[K_2]$ is a quadratic function of the transverse generalized displacements, $\{q_w\}$. The non-linearity is thus of the cubic type and the system of equations (14) is a system of Duffing equations.

The damping factor β is given by

$$\beta = \alpha\omega_{l1}^2, \tag{15}$$

where ω_{l1} is the first linear resonance frequency.

2.2. HARMONIC BALANCE METHOD

The excitations considered will be of the form $\{\bar{P}\} = \{P\}\cos(\omega t)$. Numerical, experimental and analytical investigations confirm that plates vibrating with displacement amplitudes of the order of their thickness due to excitation by harmonic forces, usually experience periodic motion [29]. In this paper, only periodic motions are analyzed and the harmonic balance method will be applied.

Consequently, the steady state response $\{q_w(t)\}$ is expressed as

$$\{q_w(t)\} = \sum_{i=1,3,\ldots}^{2k-1} \{w_{ci}\}\cos(i\omega t) + \{w_{si}\}\sin(i\omega t). \tag{16}$$

Because the non-linearity is cubic, only odd harmonics are taken into account. Equation (16) is inserted into the equations of motion (14) and the coefficients of the same harmonic components are compared (thus the designation *harmonic balance*). The resulting equations of motion in the frequency domain are of the form

$$\{F\} = (-\omega^2[M] + [C] + [KL] + [KNL])\{w\} - \{P\} = \{0\}. \tag{17}$$

In equation (17), $[M]$ represents the mass matrix, $[C]$ represents the damping matrix and $[KL]$ represents the linear stiffness matrix. These matrices are constant. $[KNL]$ represents the non-linear stiffness matrix, which is formed by a combination of $[K_4]$ and $[K_2]$ and depends quadratically on the vector of generalized displacements $\{w\}^{\mathrm{T}} = \lfloor w_{c1}\ w_{s1}\ w_{c3}\ w_{s3} \ldots w_{ci}\ w_{si} \rfloor$. The high order integrals involved in calculating the matrices in equation (17) are accurately evaluated by using symbolic computation [36], which is also helpful in the application of the harmonic balance method [27].

The total number of d.o.f. of the model, n, is given by $n = 2kp_o^2$, for a damped model, or $n = kp_o^2$, for an undamped model, where k represents the number of harmonics.

The form of the matrices in equation (17) depends on the number of harmonics chosen. For example, for damped systems and when two harmonics are considered, one has

$$\{q_w(t)\} = \{w_{c1}\}\cos(\omega t) + \{w_{s1}\}\sin(\omega t) + \{w_{c3}\}\cos(3\omega t) + \{w_{s3}\}\sin(3\omega t). \tag{18}$$

By substituting expression (18) into the equations of motion (14) and neglecting harmonics higher than $3\omega t$, the following linear matrices are derived:

$$[M] = \begin{bmatrix} [M_b] & 0 & 0 & 0 \\ 0 & [M_b] & 0 & 0 \\ 0 & 0 & 9[M_b] & 0 \\ 0 & 0 & 0 & 9[M_b] \end{bmatrix}, \tag{19}$$

$$[C] = \beta \begin{bmatrix} 0 & [M_b] & 0 & 0 \\ -[M_b] & 0 & 0 & 0 \\ 0 & 0 & 0 & 3[M_b] \\ 0 & 0 & -3[M_b] & 0 \end{bmatrix}, \tag{20}$$

$$[K] = \begin{bmatrix} [K_{1b}] & 0 & 0 & 0 \\ 0 & [K_{1b}] & 0 & 0 \\ 0 & 0 & [K_{1b}] & 0 \\ 0 & 0 & 0 & [K_{1b}] \end{bmatrix}. \tag{21}$$

Also, by applying the trigonometric relations given in Appendix A, the following non-linear stiffness matrix $[KNL]$ is obtained;

$$[KNL] = \frac{1}{4}\left(\begin{bmatrix} 3[KNL_1] & 0 & [KNL_1] & 0 \\ 0 & [KNL_1] & 0 & [KNL_1] \\ [KNL_1] & 0 & 2[KNL_1] & 0 \\ 0 & [KNL_1] & 0 & 2[KNL_1] \end{bmatrix} \right.$$

$$+ \begin{bmatrix} 0 & 2[KNL_2] & 0 & 2[KNL_2] \\ 2[KNL_2] & 0 & -2[KNL_2] & 0 \\ 0 & -2[KNL_2] & 0 & 0 \\ 2[KNL_2] & 0 & 0 & 0 \end{bmatrix}$$

$$+ \begin{bmatrix} 2[KNL_3] & 0 & 4[KNL_3] & 0 \\ 0 & -2[KNL_3] & 0 & 0 \\ 4[KNL_3] & 0 & 0 & 0 \\ 0 & 0 & 0 & 0 \end{bmatrix}$$

$$+ \begin{bmatrix} 0 & 2[KNL_4] & 0 & 4[KNL_4] \\ 2[KNL_4] & 0 & 0 & 0 \\ 0 & 0 & 0 & 0 \\ 4[KNL_4] & 0 & 0 & 0 \end{bmatrix}$$

$$\left. + \begin{bmatrix} [KNL_5] & 0 & -[KNL_5] & 0 \\ 0 & 3[KNL_5] & 0 & -[KNL_5] \\ -[KNL_5] & 0 & 2[KNL_5] & 0 \\ 0 & -[KNL_5] & 0 & 2[KNL_5] \end{bmatrix} \right]$$

$$+\begin{bmatrix} 0 & -2[KNL_6] & 0 & 0 \\ -2[KNL_6] & 0 & 4[KNL_6] & 0 \\ 0 & 4[KNL_6] & 0 & 0 \\ 0 & 0 & 0 & 0 \end{bmatrix}$$

$$+\begin{bmatrix} 2[KNL_7] & 0 & 0 & 0 \\ 0 & -2[KNL_7] & 0 & 4[KNL_7] \\ 0 & 0 & 0 & 0 \\ 0 & 4[KNL_7] & 0 & 0 \end{bmatrix}$$

$$+\begin{bmatrix} 2[KNL_8] & 0 & 0 & 0 \\ 0 & 2[KNL_8] & 0 & 0 \\ 0 & 0 & 3[KNL_8] & 0 \\ 0 & 0 & 0 & [KNL_8] \end{bmatrix}$$

$$+\begin{bmatrix} 0 & 0 & 0 & 0 \\ 0 & 0 & 0 & 0 \\ 0 & 0 & 0 & 2[KNL_9] \\ 0 & 0 & 2[KNL_9] & 0 \end{bmatrix}$$

$$+\begin{bmatrix} 2[KNL_{10}] & 0 & 0 & 0 \\ 0 & 2[KNL_{10}] & 0 & 0 \\ 0 & 0 & [KNL_{10}] & 0 \\ 0 & 0 & 0 & 3[KNL_{10}] \end{bmatrix}\Bigg). \quad (22)$$

The matrices $[KNL_i]$ are of the form

$$[KNL_i](\{w_c\},\{w_c^*\})] = [K_4(\{w_c\},\{w_c^*\})] - [K_2(\{w_c\})]^{\mathrm{T}}[K_{1p}]^{-1}[K_2(\{w_c^*\})] - [K_2(\{w_c^*\})]^{\mathrm{T}}[K_{1p}]^{-1}[K_2(\{w_c\})], \quad (23)$$

where $[K_4(\{w_c\},\{w_c^*\})]$ means that matrix $[K_4]$ is a quadratic function of $\{w_c\}$ and $\{w_c^*\}$. In the matrices $[KNL_1]$, $[KNL_5]$, $[KNL_8]$ and $[KNL_{10}]$, $\{w_c\} = \{w_{c1}\}$, $\{w_c\} = \{w_{s1}\}$, $\{w_c\} = \{w_{c3}\}$ and $\{w_c\} = \{w_{s3}\}$, respectively, and $\{w_c\} = \{w_c^*\}$. As for the other matrices, the following equalities hold: $\{w_c\} = \{w_{c1}\}$, $\{w_c^*\} = \{w_{s1}\}$ for $[KNL_2]$; $\{w_c\} = \{w_{c1}\}$, $\{w_c^*\} = \{w_{c3}\}$ for $[KNL_3]$; $\{w_c\} = \{w_{c1}\}$, $\{w_c^*\} = \{w_{s3}\}$ for $[KNL_4]$; $\{w_c\} = \{w_{s1}\}$, $\{w_c^*\} = \{w_{c3}\}$ for $[KNL_6]$; $\{w_c\} = \{w_{s1}\}$, $\{w_c^*\} = \{w_{s3}\}$ for $[KNL_7]$; $\{w_c\} = \{w_{c3}\}$, $\{w_c^*\} = \{w_{s3}\}$ for $[KNL_9]$.

The vector of generalized displacements is, in the two harmonics case, defined as

$$\{w\} = \begin{Bmatrix} w_{c1} \\ w_{s1} \\ w_{c3} \\ w_{s3} \end{Bmatrix}. \tag{24}$$

2.3. SOLUTION OF THE EQUATIONS OF MOTION

A continuation method originally proposed by Riks [37] and Crisfield [38] to study buckling phenomena and adopted by Lewandowski [39–41] to the study of free and forced vibration of beams will be used to solve the equations of motion (17). This method has also been applied in the study of free and steady state forced harmonic vibration [27, 28] and of periodic, multi-harmonic free vibration [19, 20] of isotropic and composite laminated plates.

The continuation method is composed of two main loops. In the external loop, a predictor to the solution is defined, using the two last determined points of the backbone curve. In the internal loop, the approximated solution is corrected by applying Newton's method to equation (17), considering variations not only in the generalized co-ordinate but also in the frequency of vibration. Thus, the following equation is solved:

$$[J]\{\delta w\} - [M]\{w\}\,\delta\omega^2 = -\{F\}. \tag{25}$$

$\{\delta w\}$ and $\delta\omega^2$ represent, respectively, the corrections of the vector of generalized displacements and of the square of the frequency of vibration.

In equation (25) there are n variables and $n + 1$ unknowns, and another equation is needed. Turning points of the backbone curve are passed as long as an adequate parameter is chosen. The parameter adopted is the arc-length s, which is obtained by constraining the distance between the two successive points of the FRF curve to a fixed value by the constraint equation

$$s^2 = \| \Delta\{w\} \|^2. \tag{26}$$

The iterations are repeated until the inequalities

$$|\delta\omega^2/\omega^2| < error\,1, \qquad \|\{\delta w\}\|/\|\{w\}\| < error\,2, \qquad \|\{F\}\| < error\,3, \tag{27–29}$$

are satisfied

Matrix $|J|$ in equation (25) is the Jacobian matrix, defined as

$$[J] = \partial\{F\}/\partial\{w\}. \tag{30}$$

From equation (17), it results that $[J]$ is

$$[J] = -\omega^2[M] + [C] + [KL] + \partial[KNL]\{w\}/\partial\{w\}. \tag{31}$$

By applying variations, it can be demonstrated that [29]

$$d([KNL]\{w\}) = (3[KNL^{K4}] + 2[KNL^{K2}])d\{w\} + d[KNL^{K2}]\{w\}, \tag{32}$$

where $[KNL^{K4}]$ represents the parts of $[KNL]$ related to $[K_4]$, and $[KNL^{K2}]$ represents the parts of $[KNL]$ related to $[K_2]$.

In order to have an explicit expression for the Jacobian matrix, the following approximation will be used:

$$d[KNL^{K2}]\{w\} \cong [KNL^{K2}]d\{w\}. \tag{33}$$

Thus one has

$$\partial[KNL]\{w\}/\partial\{w\} \cong 3[KNL] \tag{34}$$

and

$$[J] \cong -\omega^2[M] + [C] + [KL] + 3[KNL]. \tag{35}$$

If the middle-plan in-plane displacements are not included in the model, $[K_2]$ does not exist and the former approximations are exact.

In the resolution of non-linear systems by Newton-type methods, the Jacobian may be unknown or may be very time-consuming to update in each iteration. Thus, it is common to use approximations to the Jacobian instead of the Jacobian itself [42, 43]. As the error criteria must be satisfied, the solution obtained with an approximated Jacobian is still accurate. In this particular case, it is important to verify if the equilibrium equations are satisfied, as is done in equation (29).

3. CONVERGENCE STUDIES

It is intended to demonstrate that the model presented requires a small number of degrees of freedom for accuracy. Therefore, the convergence of the steady state

TABLE 1

Linear natural frequencies (rad/s) ($p_o = 7$)

Mode	1	2	3	4	5	6	7
Plate 1	579·442	1134·75	1227·31	1741·64	2011·37	2232·23	2587·96
Plate 2	763·097	1419·93	1647·38	2219·17	2650·82	2865·34	3194·66

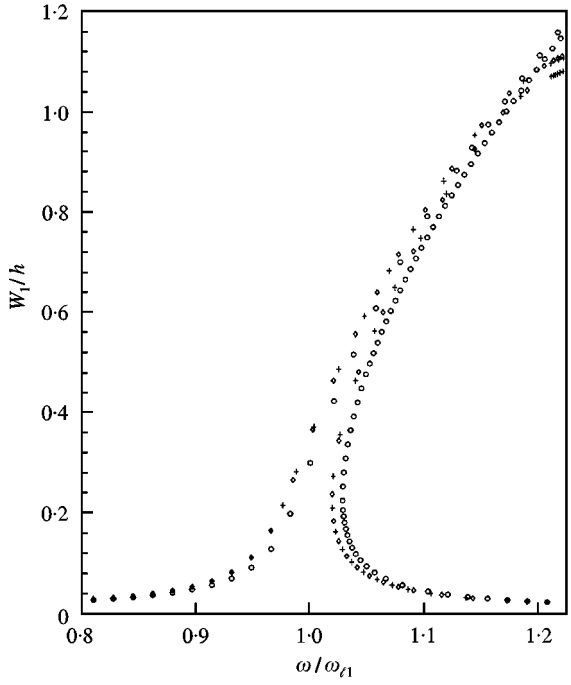

Figure 2. Amplitude of first harmonic of Plate 1 calculated with: ○, 1 harmonic; ◇, 2 harmonics; +, three harmonics; at $(\xi, \eta) = (0, 0)$. $p_o = 5$, $p_i = 8$.

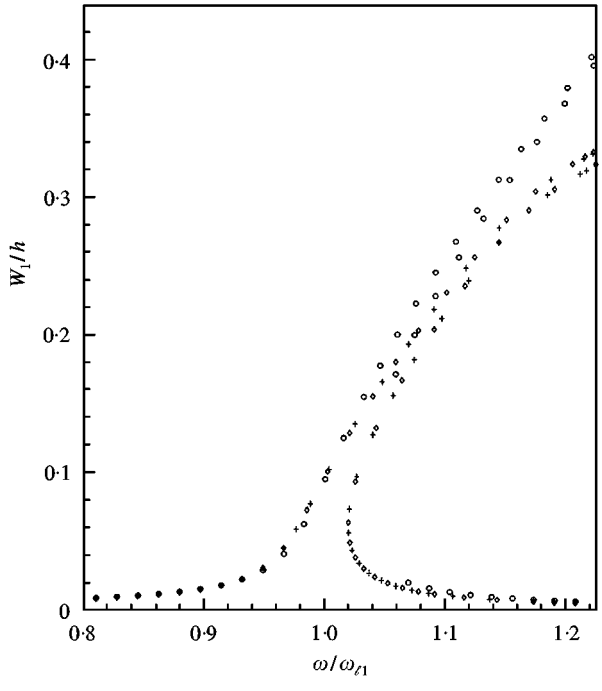

Figure 3. Amplitude of first harmonic of Plate 1 calculated with: ○, 1 harmonic; ◇, 2 harmonics; +, three harmonics; at $(\xi, \eta) = (0{\cdot}5, 0{\cdot}5)$. $p_o = 5$, $p_i = 8$.

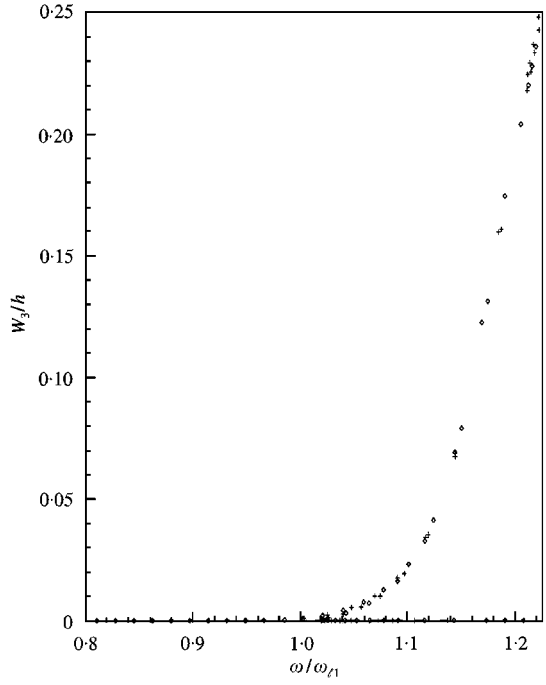

Figure 4. Amplitude of third harmonic of Plate 1 calculated with: ◇, 2 harmonics; +, three harmonics; at $(\xi, \eta) = (0, 0)$. $p_o = 5$, $p_i = 8$.

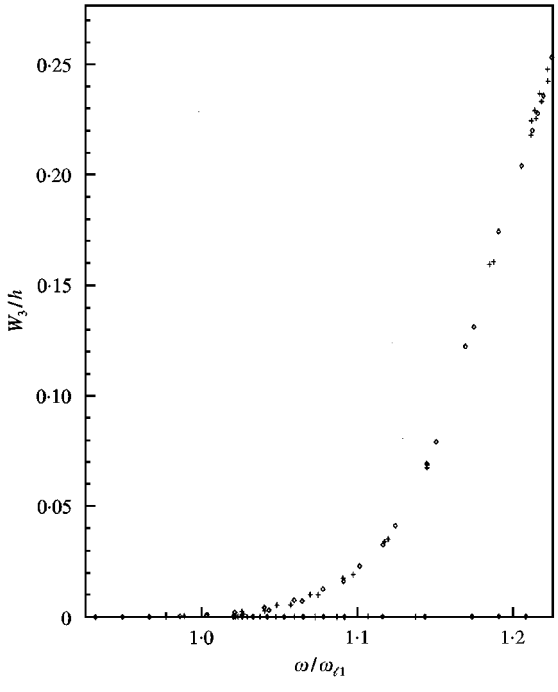

Figure 5. Amplitude of third harmonic of Plate 1 calculated with: ◇, 2 harmonics; +, three harmonics; at $(\xi, \eta) = (0{\cdot}5, 0{\cdot}5)$. $p_o = 5$, $p_i = 8$.

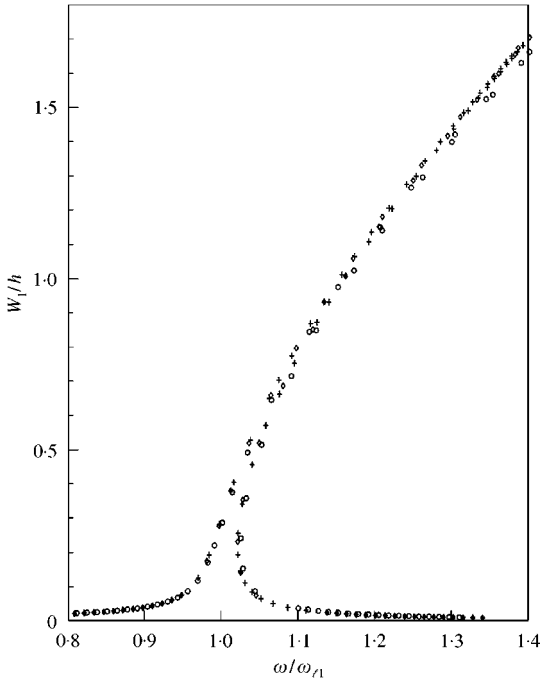

Figure 6. Amplitude of first harmonic of Plate 2 calculated with: ○, 1 harmonic; ◇, 2 harmonics; +, three harmonics; at $(\xi, \eta) = (0, 0)$. $p_o = 5$, $p_i = 10$.

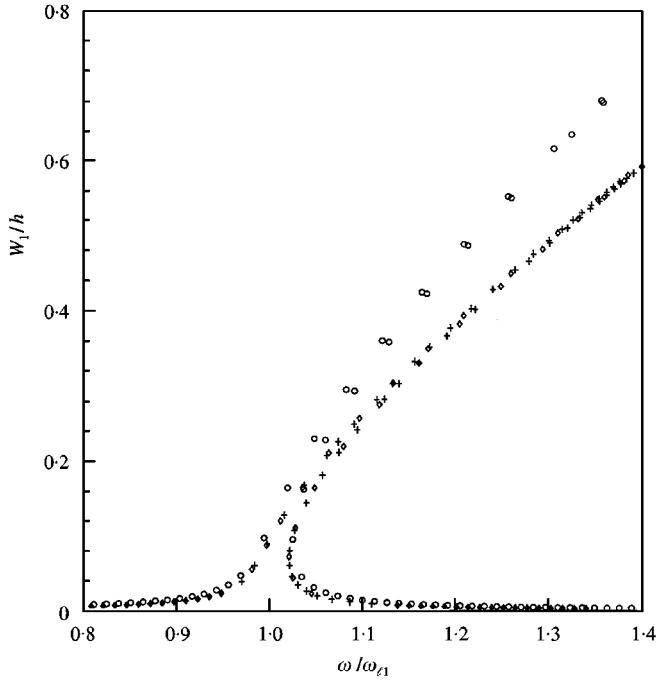

Figure 7. Amplitude of first harmonic of Plate 2 calculated with: ○, 1 harmonic; ◇, 2 harmonics; +, three harmonics; at $(\xi, \eta) = (0{\cdot}5, 0{\cdot}5)$. $p_o = 5$, $p_i = 10$.

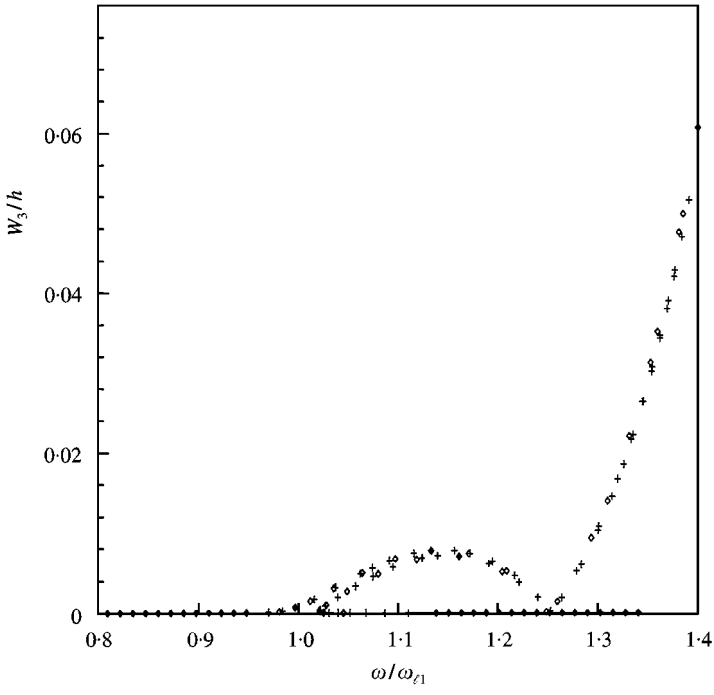

Figure 8. Amplitude of third harmonic of Plate 2 calculated with: ◇, 2 harmonics; +, three harmonics; at $(\xi, \eta) = (0, 0)$. $p_o = 5$, $p_i = 10$.

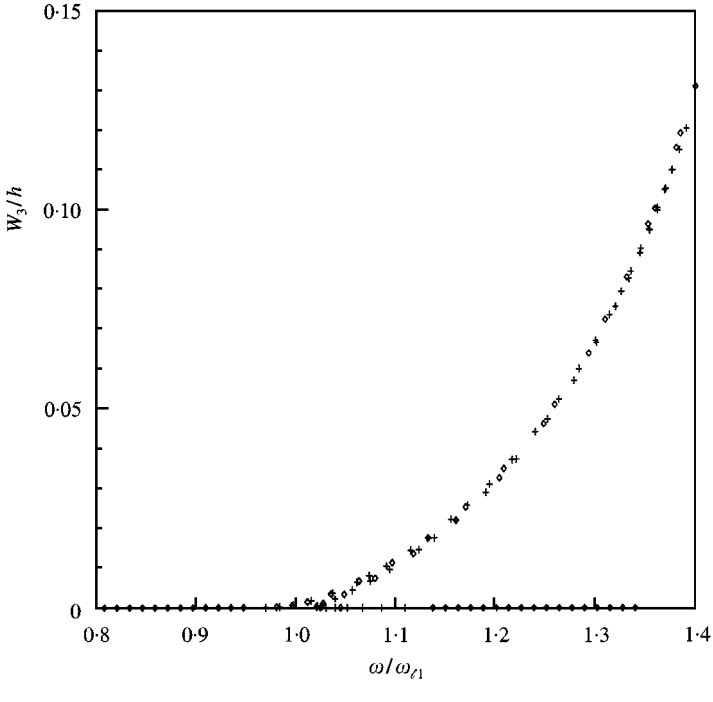

Figure 9. Amplitude of third harmonic of Plate 2 calculated with: ◇, 2 harmonics; +, three harmonics; at $(\xi, \eta) = (0{\cdot}5, 0{\cdot}5)$. $p_o = 5$, $p_i = 10$.

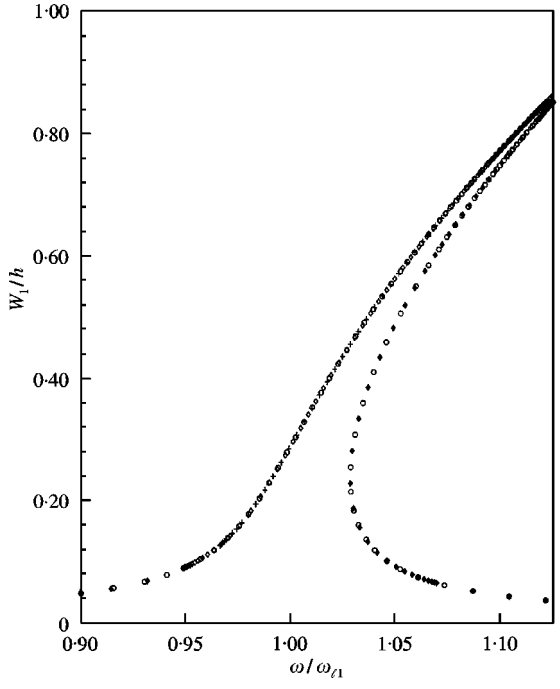

Figure 10. Amplitude of first harmonic of Plate 1 calculated with $p_i = 10$ and: ○, $p_o = 5$; ◇, $p_o = 6$; +, $p_o = 7$ $(\xi, \eta) = (0, 0)$.

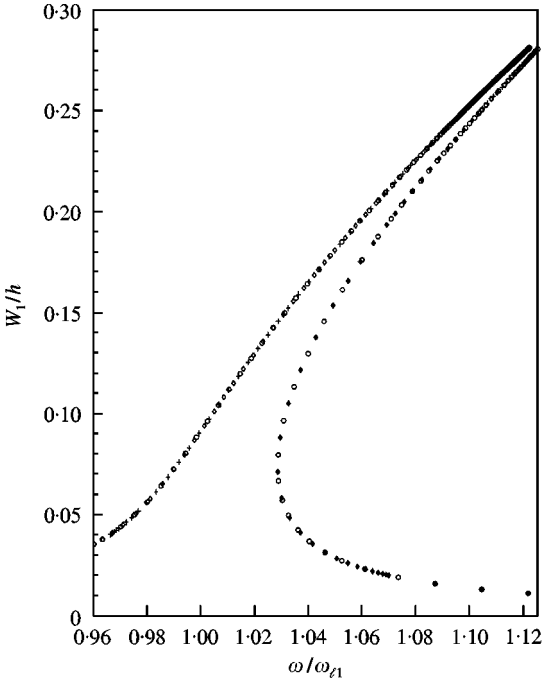

Figure 11. Amplitude of first harmonic of Plate 1 calculated with $p_i = 10$ and: ○, $p_o = 5$; ◇, $p_o = 6$; +, $p_o = 7$. $(\xi, \eta) = (0{\cdot}5, 0{\cdot}5)$.

solutions with the number of harmonics and with the number of shape functions is investigated in the next sections.

Two plates are studied, one is isotropic (aluminium DTDSO 70)—Plate 1—and the other is a composite laminated plate (graphite/epoxy)—Plate 2. Plate 1 has the dimensions $a = 300$ mm, $b = 320$ mm, $h = 1$ mm, and the material properties $E = 7 \times 10^{10}$ N/m^2, $\rho = 2778$ kg/m^3, $v = 0{\cdot}34$. Plate 2 has five layers, with the following orientation of principal axes (45°, $-45°$, 45°, $-45°$, 45°). Its dimensions are $a = 300$ mm, $b = 300$ mm, $h = 1$ mm, and each layer has the material properties $E_L = 173{\cdot}0$ GN/m^2, $E_T = E_L/15{\cdot}4$ GN/m^2, $G_{LT} = 0{\cdot}79 \quad E_T$ GN/m^2, $v_{LT} = 0{\cdot}3$, $\rho = 1540$ kg/m^3.

Aluminium is generally used in commercially aircraft and composite laminated plates are more widely used in military aircraft, particularly in smaller size planes [44].

The linear natural frequencies of both plates are given in Table 1.

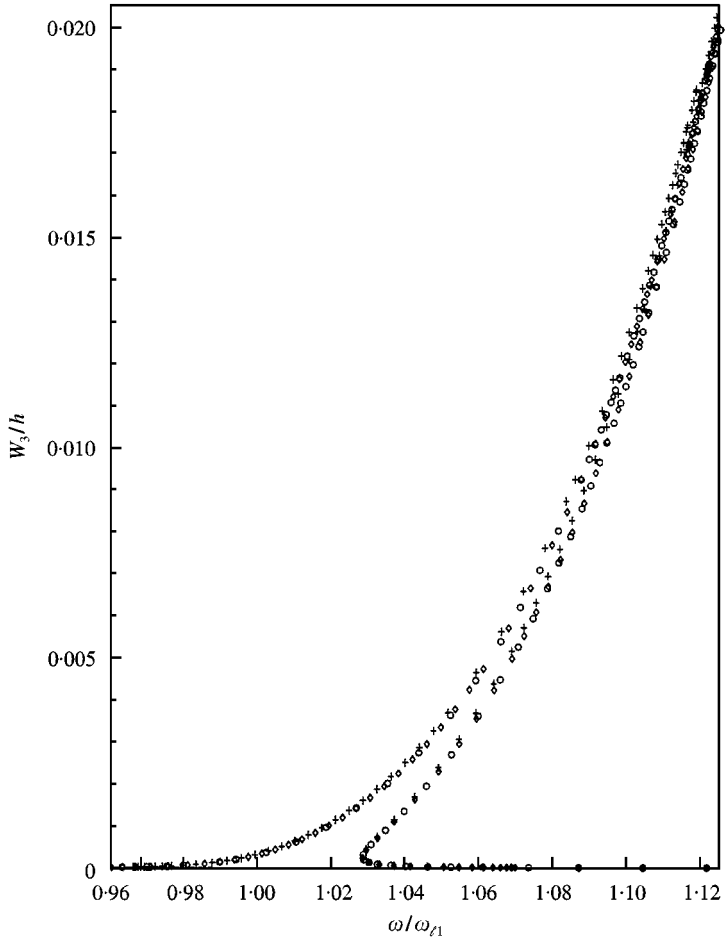

Figure 12. Amplitude of third harmonic of Plate 1 calculated with $p_i = 10$ and: ○, $p_o = 5$; ◇, $p_o = 6$; +, $p_o = 7$ $(\xi, \eta) = (0, 0)$.

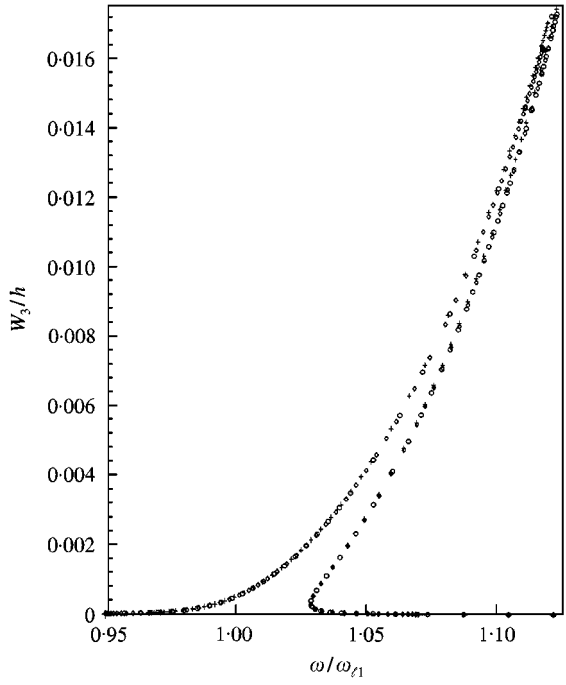

Figure 13. Amplitude of third harmonic of Plate 1 calculated with $p_i = 10$ and: ○, $p_o = 5$; ◇, $p_o = 6$; +, $p_o = 7$. $(\xi, \eta) = (0{\cdot}5, 0{\cdot}5)$.

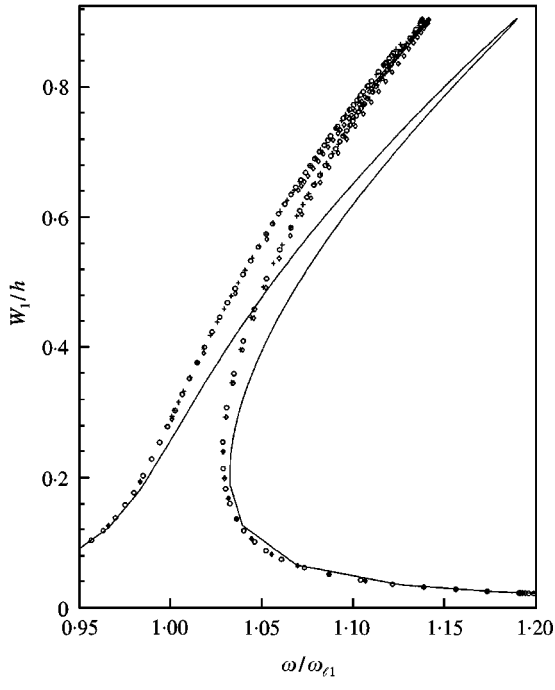

Figure 14. Amplitude of first harmonic of Plate 1 calculated with $(\xi, \eta) = (0, 0)$ with $p_o = 5$ and: − $p_i = 0$; ◇, $p_i = 5$; +, $p_i = 8$; ○, $p_i = 10$.

3.1. CONVERGENCE WITH THE NUMBER OF HARMONICS

The convergence of the frequency response functions of Plates 1 and 2 with the number of harmonics used in equation (16) is investigated. The plates are excited by a harmonic plane wave at normal incidence and damping is neglected. The mass matrix $[M]$, the linear stiffness matrix $[KL]$ and the non-linear stiffness matrix $[KNL]$ are explicitly given in references [19, 20].

The amplitudes of the first and third harmonics are given by the expressions

$$W_1 = \sqrt{w_{c1}^2 + w_{s1}^2}, \qquad W_3 = \sqrt{w_{c3}^2 + w_{s3}^2}, \tag{36, 37}$$

where w_{c1}, w_{s1}, w_{c3} and w_{s3} are, in this order, the amplitudes of the cosine and sine terms of the first and third harmonics. Thus, W_1 and W_3 are always positive. The sine terms are zero in the case of undamped vibration.

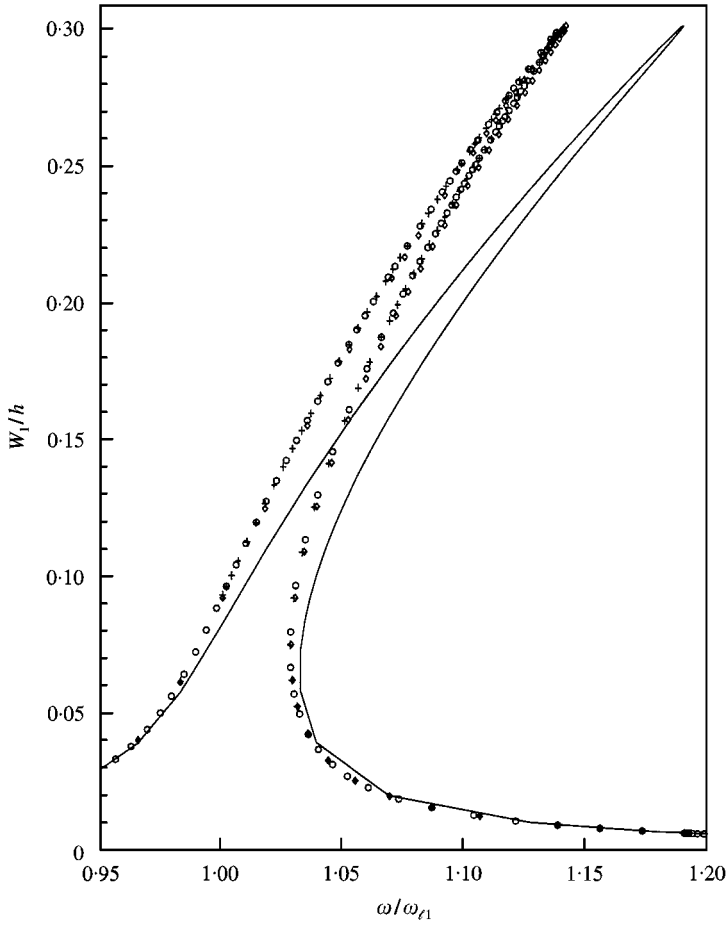

Figure 15. Amplitude of first harmonic of Plate 1 calculated with $(\xi, \eta) = (0{\cdot}5, 0{\cdot}5)$ with $p_o = 5$ and: $-$ $p_i = 0$; $\diamond$, $p_i = 5$; $+$, $p_i = 8$; $\circ$, $p_i = 10$.

Plate 1 was excited with a wave of 5 N/m^2 amplitude. Figures 2–5 show the variation of the amplitude of the first and third harmonics with frequency (i.e., the frequency response functions (FRF) of the first and third harmonics). The amplitudes were calculated at the points indicated by the non-dimensional co-ordinates (ξ, η). The one-harmonic approximation gives remarkably poor results: its solutions deviate from the two- and three-harmonic solutions when the frequency of vibration approaches the first natural frequency and for quite low amplitudes, as shown in Figures 2 and 3. Moreover, it neglects the third harmonic which attains quite large vibration amplitudes: Figures 4 and 5. When using two and three harmonics in the time series, almost coincident results are obtained. Therefore, a model with two harmonics will be used in the study of Plate 1.

Figures 6–9 show the frequency-response functions of the first and third harmonics of Plate 2, when this is excited by a wave with 4 N/m^2 amplitude. Under these conditions, the one harmonic approximation gives a reasonable approximation for the amplitude of vibration of the plate at point $(\xi, \eta) = (0, 0)$ and a bad approximation for the amplitude of vibration at point $(\xi, \eta) = (0{\cdot}5, 0{\cdot}5)$. In this last point, the one-harmonic solution deviates from the two- and three-harmonics solutions as soon as the frequency of vibration approaches the first natural frequency and for quite low amplitudes. With two and three harmonics, similar results were obtained and two harmonics will be used in the following analyses of Plate 2.

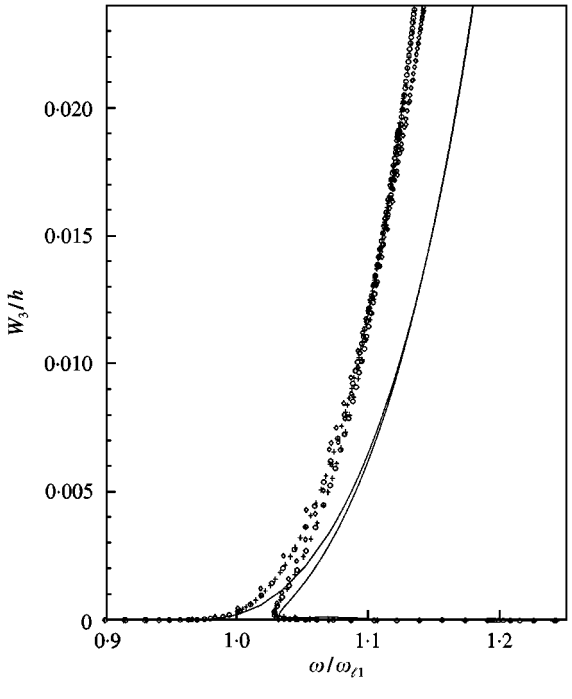

Figure 16. Amplitude of third harmonic of Plate 1 calculated with $(\xi, \eta) = (0, 0)$ with $p_o = 5$ and: $-$ $p_i = 0$; $\diamond$, $p_i = 5$; $+$, $p_i = 8$; $\circ$, $p_i = 10$.

Although two harmonics were enough for convergence in the present analysis, it should be pointed out that if the excitation has a component similar to a higher order mode with a natural frequency near k times the first resonance frequency, this mode may be excited due to internal resonance. In this case, as suggested in reference [45], it may be necessary to include the kth harmonic in the time series. Internal resonance is discussed in the second part of this paper.

3.2. CONVERGENCE WITH THE NUMBER OF SHAPE FUNCTIONS

The FRFs of Plate 1 due to a harmonic excitation at normal incidence with an amplitude of 5 N/m^2 were calculated by using different numbers of out-of-plane and in-plane shape functions. The damping factor β was calculated by expression (15) with $\alpha = 0{\cdot}01$.

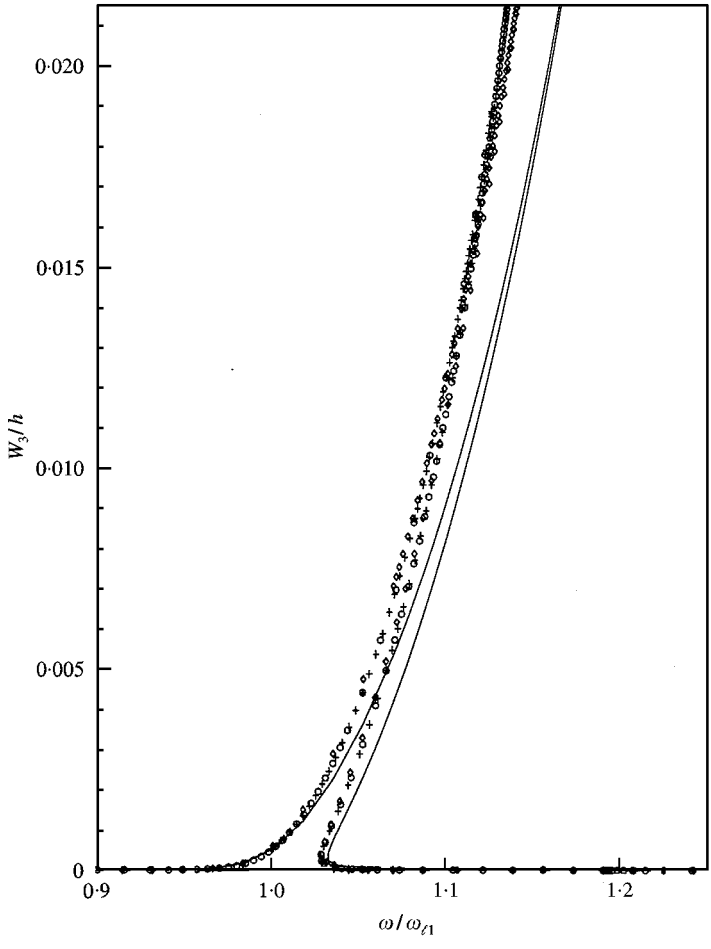

Figure 17. Amplitude of third harmonic of Plate 1 calculated with $(\xi, \eta) = (0{\cdot}5, 0{\cdot}5)$ with $p_o = 5$ and: $-$ $p_i = 0$; $\diamond$, $p_i = 5$; $+$, $p_i = 8$; $\circ$, $p_i = 10$.

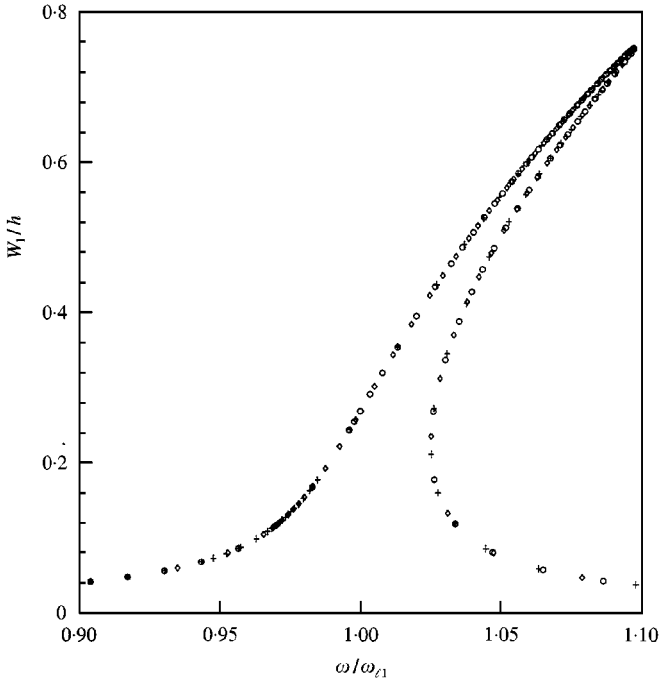

Figure 18. Amplitude of first harmonic of Plate 2 calculated with $p_o = 10$ and: ○, $p_o = 5$; ◇, $p_o = 6$; +, $p_o = 7$. $(\xi, \eta) = (0, 0)$.

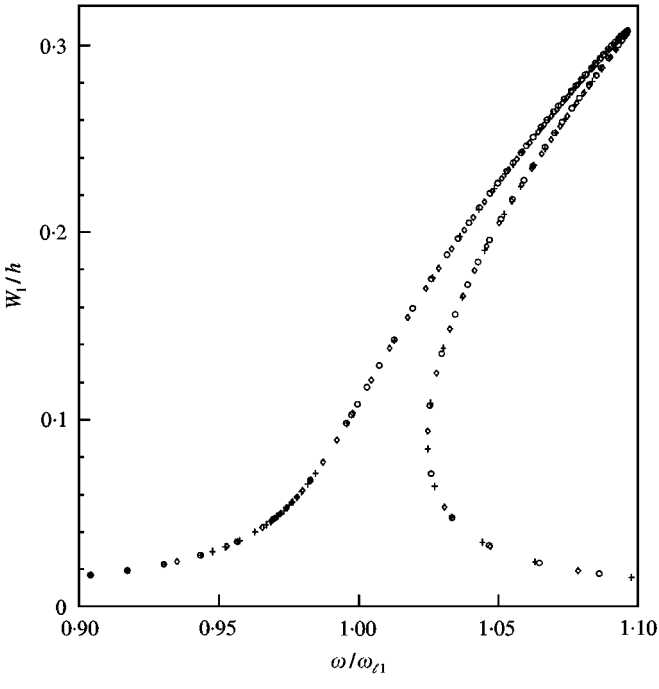

Figure 19. Amplitude of first harmonic of Plate 2 calculated with $p_i = 10$ and: ○, $p_o = 5$; ◇, $p_o = 6$; +, $p_o = 7$. $(\xi, \eta) = (0{\cdot}5, 0{\cdot}5)$.

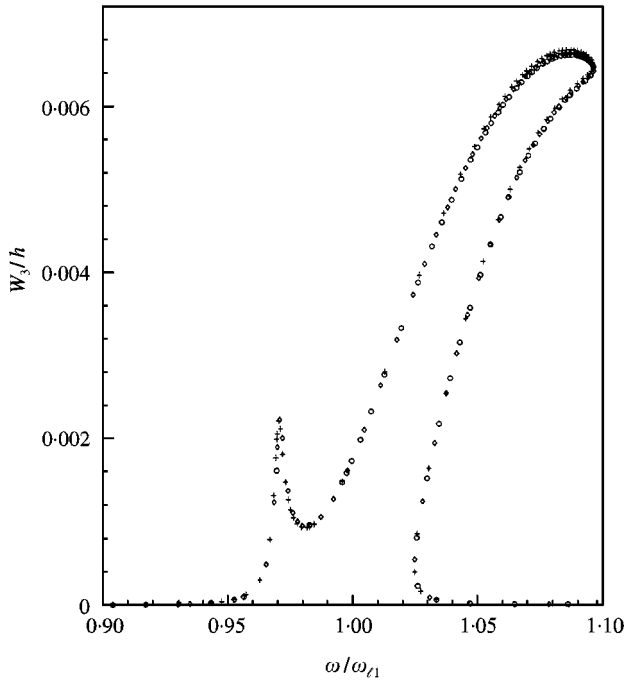

Figure 20. Amplitude of third harmonic of Plate 2 calculated with $p_i = 10$ and: ○, $p_o = 5$; ◇, $p_o = 6$; +, $p_o = 7$. $(\xi, \eta) = (0, 0)$.

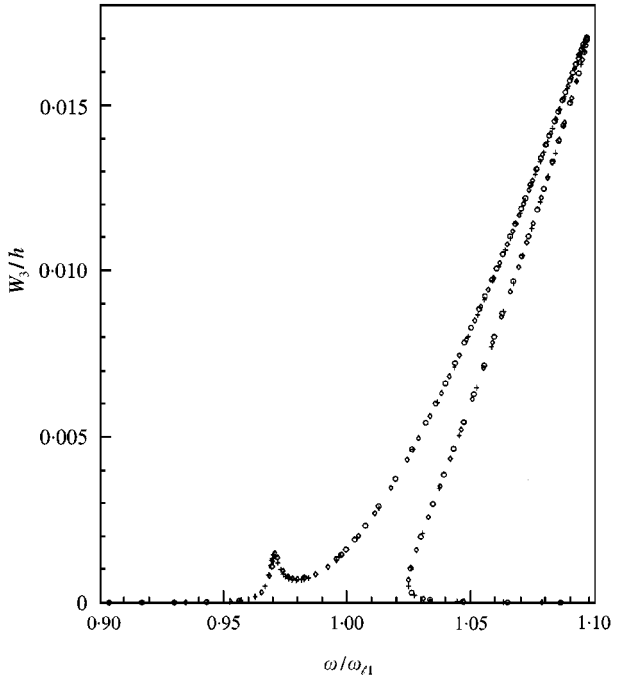

Figure 21. Amplitude of third harmonic of Plate 2 calculated with $p_i = 10$ and: ○, $p_o = 5$; ◇, $p_o = 6$; +, $p_o = 7$. $(\xi, \eta) = (0{\cdot}5, 0{\cdot}5)$.

In Figures 10–13 the FRFs obtained with different number of out-of-plane shape functions are compared. Ten in-plane shape functions were used in all the models. Five out-of-plane shape functions, i.e., 100 d.o.f., provide an exact approximation of the first harmonic and a very good approximation of the third harmonic.

In Figures 14–17, the FRFs obtained with different number of in-plane shape functions are compared. The exclusion of the middle-plane in-plane displacements ($p_i = 0$), makes the hardening spring effect of both harmonics more severe. Five in-plane shape functions give accurate values for the first harmonic. The third harmonic is approximately well calculated with five in-plane shape functions, and very accurately calculated with eight in-plane shape functions.

The FRFs of Plate 2 due to a harmonic excitation at normal incidence with an amplitude of 4 N/m^2 were calculated by using different numbers of out-of-plane and in-plane shape functions. The damping factor β was calculated by expression (15) with $\alpha = 0{\cdot}01$.

In Figures 18–21, the frequency-response functions of Plate 2, calculated with different numbers of out-of-plane shape functions are compared. Ten in-plane shape functions were used in all the models. With five out-of-plane shape functions, i.e., 100 d.o.f., accurate results are obtained.

If the middle-plane in-plane displacements are not considered ($p_i = 0$), the resonance frequency increases more with the first-harmonic amplitude: see Figures 22–23. The maximum amplitude of vibration of the first harmonic is equivalent

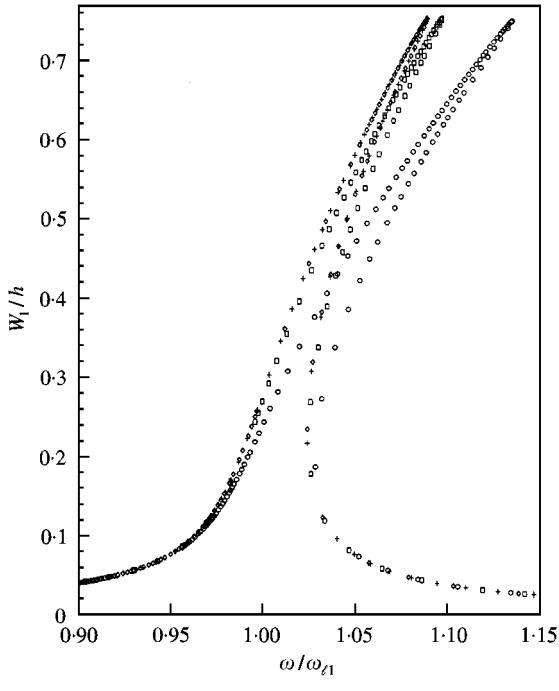

Figure 22. Amplitude of first harmonic of Plate 2 calculated with $p_o = 5$ and: ○, $p_i = 0$; □, $p_i = 7$; +, $p_i = 8$; ◇, $p_i = 10$; $(\xi, \eta) = (0, 0)$.

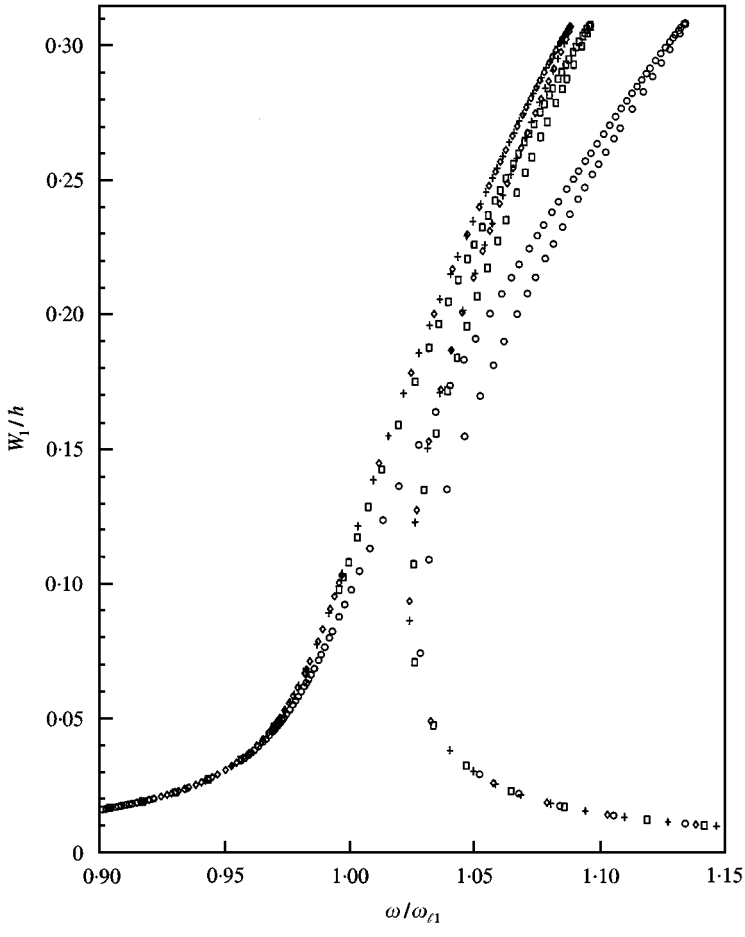

Figure 23. Amplitude of first harmonic of Plate 2 calculated with $p_o = 5$ and: ○, $p_i = 0$; □, $p_i = 7$; +, $p_i = 8$; ◇, $p_i = 10$; $(\xi, \eta) = (0{\cdot}5, 0{\cdot}5)$.

with or without middle plane in-plane displacements. Eight in-plane shape functions give accurate values for the first harmonic.

Figures 24–25 display the FRFs of the third harmonic of Plate 2 calculated with a different number of in-plane shape functions. The exclusion of the middle-plane in-plane displacements is more important in the calculation of the third harmonic than in the first. The amplitude of vibration for the third harmonic is largely overpredicted if the middle-plane in-plane displacements are neglected. The third harmonic is well calculated with seven in-plane shape functions.

4. CONCLUSIONS

A model for geometrical non-linear, steady state, multi-harmonic vibration of isotropic and composite laminated rectangular plates was developed by using the HFEM and the HBM.

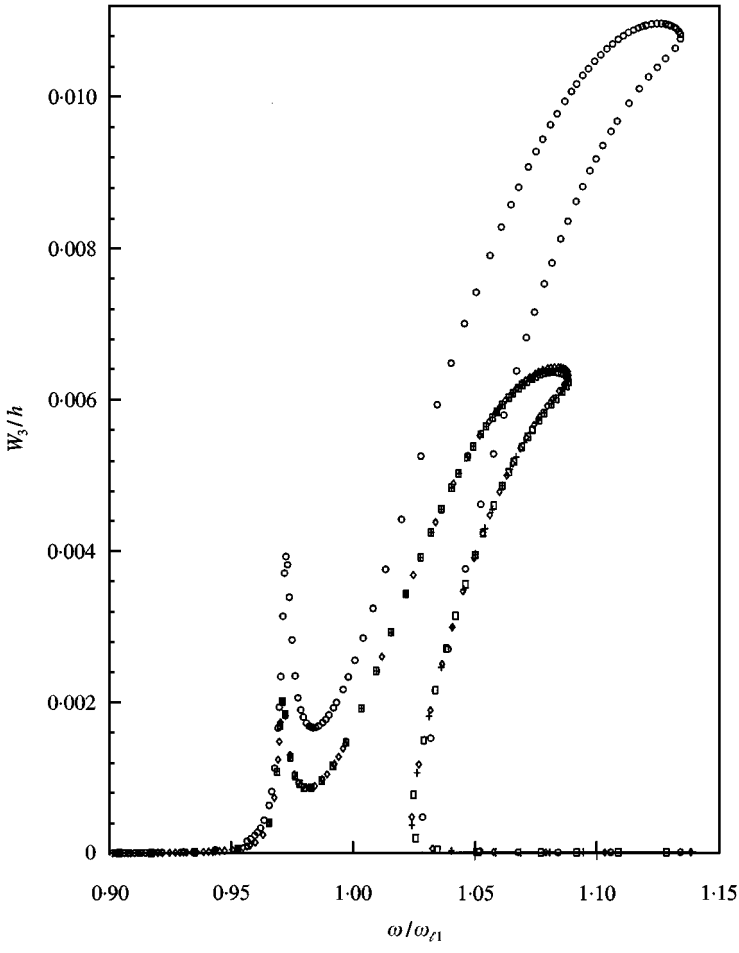

Figure 24. Amplitude of third harmonic of Plate 2 calculated with $p_o = 5$ and: ○, $p_i = 0$; □, $p_i = 7$; +, $p_i = 8$; ◇, $p_i = 10$. $(\xi, \eta) = (0, 0)$.

The convergence of the frequency-response functions with the number of harmonics was studied. The two- and three-harmonic approximations produced very similar results, indicating that the fifth and higher harmonics can be neglected in the analysis of rectangular plates excited by harmonic plane waves. However, this will not be true if a higher order mode is excited due to internal resonance.

The convergence of the frequency-response functions with the number of out-of-plane and of in-plane shape functions was investigated. More in-plane than out-of-plane shape functions are necessary for convergence. The in-plane shape functions are associated with the in-plane displacements and, therefore, their importance increases with the amplitude of vibration displacement.

The convergence studies indicate that the HFEM and HBM allow one to model the geometrical non-linear, forced, periodic vibrations of plates accurately and with a small number of d.o.f.

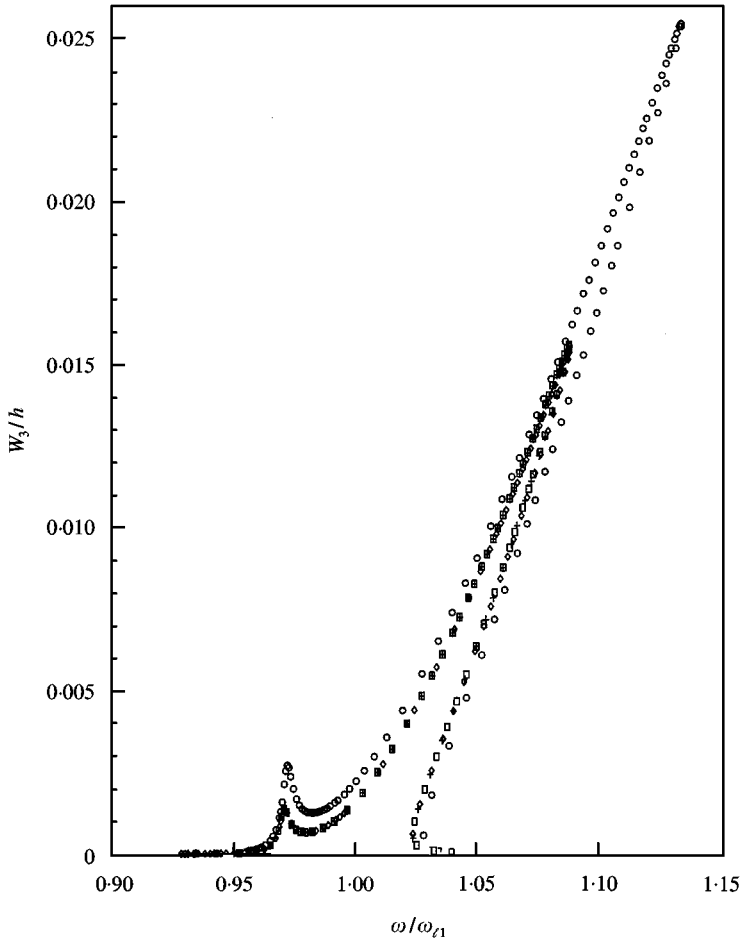

Figure 25. Amplitude of third harmonic of Plate 2 calculated with $p_o = 5$ and: ○, $p_i = 0$; □, $p_i = 7$; +, $p_i = 8$; ◇, $p_i = 10$. $(\xi, \eta) = (0{\cdot}5, 0{\cdot}5)$.

ACKNOWLEDGMENT

P. Ribeiro gratefully acknowledges the scholarship PRAXIS XXI/BD/3868/94 from the *Fundação para a Ciéncia e a Tecnologia*, Portugal.

REFERENCES

1. H. N. Chu and G. Herrmann 1956 *Transactions of the ASME, Journal of Applied Mechanics* **23**, 532–540. Influence of large amplitudes on free flexural vibrations of rectangular elastic plates.
2. P. W. Smith, C. I. Malme and C. M. Gogos 1961 *The Journal of the Acoustical Society of America* **33**, 1476–1482. Nonlinear response of a simple clamped panel.
3. M. Sathyamoorthy 1978 *Journal of Sound and Vibration* **58**, 301–304. Nonlinear vibration of rectangular plates.
4. C. Y. Chia 1980 *Nonlinear Analysis of Plates*. New York: McGraw-Hill.

5. H. Eslami and O. A. Kandil 1989 *American Institute of Aeronautics and Astronautics Journal* **27**, 955–960. Nonlinear forced vibration of orthotropic rectangular plates using the method of multiple scales.
6. H. Eslami and O. A. Kandil 1989 *American Institute of Aeronautics and Astronautics Journal* **27**, 961–967. Two-mode nonlinear vibration of orthotropic plates using the method of multiple scales.
7. A. Y. Leung and S. G.Mao 1995 *Journal of Sound and Vibration* **183**, 475–491. A symplectic Galerkin method for non-linear vibration of beams and plates.
8. R. Lewandowski 1996 *Meccanica* **31**, 323–346. On beams membranes and plates vibration backbone curves in cases of internal resonance.
9. B. Abe, Y. Kobayashi and G. Yamada 1998 *International Journal of Non-Linear Mechanics* **33**, 675–690. Two-mode response of simply supported, rectangular laminated plates.
10. Y. Shi and C. Mei 1996 *Journal of Sound and Vibration* **193**, 453–464. A finite element time domain modal formulation for large amplitude free vibration of beams and plates.
11. Y. Shi, R. Y. Y. Lee and C. Mei 1997 *American Institute of Aeronautics and Astronautics Journal* **35**, 159–166. Finite element method for nonlinear free vibrations of composite plates.
12. R. Benamar, M. M. K. Bennouna and R. G. White 1993 *Journal of Sound and Vibration* **164**, 295–316. The effects of large vibration amplitudes on the mode shapes and natural frequencies of thin elastic structures. Part II: fully clamped rectangular isotropic plates.
13. R. Benamar, M. M. K. Bennouna and R. G. White 1994 *Journal of Sound and Vibration* **175**, 377–395. The effects of large vibration amplitudes on the mode shapes and natural frequencies of thin elastic structures. Part III: fully clamped rectangular isotropic plates-measurements of the mode shape amplitude dependence and the spatial distribution of harmonic distortion.
14. W. Han, 1993 *Ph.D. Thesis*, *University of Southampton*, The analysis of isotropic and laminated rectangular plates including geometrical non-linearity using the *p*-version finite element method.
15. W. Han and M. Petyt 1997 *Computers and Structures* **63**, 295–308. Geometrically nonlinear vibration analysis of thin, rectangular plates using the hierarchical finite element method—I: the fundamental mode of isotropic plates.
16. W. Han and M. Petyt 1997 *Computers and Structures* **63**, 309–318. Geometrically nonlinear vibration analysis of thin, rectangular plates using the hierarchical finite element method—II: 1st mode of laminated plates and higher modes of isotropic and laminated plates.
17. S. L. Lau, Y. K. Cheung and S. Y. Wu 1984 *Transactions of the ASME*, *Journal Applied Mechanics* **51**, 837–844. Nonlinear vibration of thin elastic plates. Part 1: generalized incremental Hamilton's principle and element formulation.
18. S. L. Lau, Y. K. Cheung and S. Y. Wu 1984 *Transactions of the ASME*, *Journal of Applied Mechanics* **51**, 845–851. Nonlinear vibration of thin elastic plates. Part 2: Internal resonance by amplitude-incremental finite element.
19. P. Ribeiro and M. Petyt *International Journal of Non-linear Mechanics* Nonlinear free vibration of isotropic plates with internal resonance (accepted).
20. P. Ribeiro and M. Petyt *Journal of Sound and Vibration* Multi-modal geometrical nonlinear free vibration of composite laminated plates (accepted).
21. C. Mei 1973 *Computers and Structures* **3**, 163–174. Finite element displacement method for large amplitude free flexural vibration of beams and plates.
22. C. Mei and K. Decha-Umphai 1985 *American Institute of Aeronautics and Astronautics Journal* **23**, 1104–1110. A finite element method for non-linear forced vibrations of rectangular plates.

23. S. R. Rao, A. H. Sheikh and M. Mukhopadhyay 1993 *Journal of the Acoustical Society of America* **93**, 3250–3257. Large-amplitude finite element flexural vibration of plates/stiffened plates.
24. J. N. Reddy and W. C. Chao 1981 *Computers and Structures* **13**, 341–347. Large-deflection and large-amplitude free vibrations of laminated composite-material plates.
25. M. Ganapathi, T. K. Varadan and B. S. Sarma 1991 *Computers and Structures* **39**, 685–688. Nonlinear flexural vibrations of laminated orthotropic plates.
26. C. K. Chiang, C. Mei and C. E. Graÿ 1991 *Transactions of the ASME journal of Vibration and Acoustics* **113**, 309–315. Finite element large-amplitude free and forced vibrations of rectangular thin composite plates.
27. P. Ribeiro and M. Petyt *International Journal of Mechanical Sciences* **41**, 437–459. Nonlinear vibration of plates by the hierarchical finite element and continuation methods.
28. P. Ribeiro and M. Petyt *Composite Structures*. Nonlinear vibration of composite laminated plates by the hierarchical finite element method (accepted).
29. P. Ribeiro 1998 *Ph.D. Thesis, University of Southampton*. Geometrical nonlinear vibration of beams and plates by the hierarchical finite element method.
30. W. Szemplinska-Stupnicka 1990 *The Behaviour of Non-linear Vibrating Systems*. Dordrecht: Kluwer Academic Publishers.
31. R. E. Mickens 1984 *Journal of Sound and Vibration* **94**, 456–460. Comments on the method of harmonic balance.
32. M. N,. Hamdan and T. D. Burton 1993 *Journal of Sound and Vibration* **166**, 255–266. On the steady state response and stability of non-linear oscillators using harmonic balance.
33. R. Seydel 1988 *From Equilibrium to Chaos. Practical Bifurcation and Stability Analysis*. New York: Elsevier Science.
34. P. Ribeiro and M. Petyt *Journal of Sound and Vibration* Geometrical nonlinear, steady-state, forced, periodic vibration of plates. Part II: Stability study and analysis of multi-modal, multi-frequency response (accepted).
35. B. A. Szabó and I. Babuska 1991 *Finite Element Analysis*. New York: John Wiley and Sons.
36. D. Redfern 1994 *The Maple Handbook*. New York: Springer-Verlag.
37. E. Riks 1979 *International Journal of Solids and Structures* **15**, 529–551. An incremental approach to the solution of snapping and buckling problems.
38. M. A. Crisfield 1981 *Computers and Structures* **13**, 55–62. A fast incremental/iterative solution procedure that handles "snap-through".
39. R. Lewandowski 1994 *Journal of Sound and Vibration* **170**, 577–593. Non-linear free vibrations of beams by the finite element and continuation methods.
40. R. Lewandowski 1997 *International Journal Solids and Structures* **34**, 1925–1947. Computational formulation for periodic vibration of geometrically nonlinear structures—Part 1: theoretical background.
41. R. Lewandowski 1997 *International Journal Solids and Structures* **34**, 1949–1964. Computational formulation for periodic vibration of geometrically nonlinear structures—Part 2: numerical strategy and examples.
42. O. C. Zienkiewicz and R. L. Taylor 1988. *The Finite Element Method*. London: McGraw-Hill, fourth edition.
43. S. Conte and C. de Boor 1987 *Elementary Numerical Analysis. An Algorithmic Approach*. Auckland: McGraw-Hill, third edition.
44. M. M. Schwartz 1992 *Composite Materials Handbook*. New York: McGraw-Hill, second edition.
45. A. Y. T. Leung and T. C. Fung 1989 *International Journal for Numerical Methods in Engineering* **28**, 1599–1618. Non-linear steady state vibration of frames by finite element method.

APPENDIX A: TRIGONOMETRIC RELATIONS

$$\cos^3(\omega t) = \tfrac{3}{4}\cos(\omega t) + \tfrac{1}{4}\cos(3\omega t) \tag{A1}$$

$$\cos^2(\omega t)\cos(3\omega t) = \tfrac{1}{4}\cos(\omega t) + \tfrac{1}{2}\cos(3\omega t) + \tfrac{1}{4}\cos(5\omega t) \tag{A2}$$

$$\cos(\omega t)\cos^2(3\omega t) = \tfrac{1}{2}\cos(\omega t) + \tfrac{1}{4}\cos(5\omega t) + \tfrac{1}{4}\cos(7\omega t) \tag{A3}$$

$$\cos^3(\omega t) = \tfrac{3}{4}\cos(3\omega t) + \tfrac{1}{4}\cos(9\omega t) \tag{A4}$$

$$\cos^2(\omega t)\sin(\omega t) = \tfrac{1}{4}\sin(\omega t) + \tfrac{1}{4}\sin(3\omega t) \tag{A5}$$

$$\cos(\omega t)\sin^2(\omega t) = \tfrac{1}{4}\cos(\omega t) - \tfrac{1}{4}\cos(3\omega t) \tag{A6}$$

$$\cos^2(\omega t)\sin(3\omega t) = \tfrac{1}{4}\sin(\omega t) + \tfrac{1}{2}\sin(3\omega t) + \tfrac{1}{4}\sin(5\omega t) \tag{A7}$$

$$\cos(\omega t)\cos(3\omega t)\sin(\omega t) = -\tfrac{1}{4}\sin(\omega t) + \tfrac{1}{4}\sin(5\omega t) \tag{A8}$$

$$\cos(\omega t)\sin(\omega t)\sin(3\omega t) = \tfrac{1}{4}\cos(\omega t) - \tfrac{1}{4}\cos(5\omega t) \tag{A9}$$

$$\cos(\omega t)\cos(3\omega t)\sin(3\omega t) = \tfrac{1}{4}\sin(5\omega t) + \tfrac{1}{4}\sin(7\omega t) \tag{A10}$$

$$\cos(\omega t)\sin^2(3\omega t) = \tfrac{1}{2}\cos(\omega t) - \tfrac{1}{4}\cos(5\omega t) - \tfrac{1}{4}\cos(7\omega t) \tag{A11}$$

$$\sin^2(\omega t)\cos(3\omega t) = -\tfrac{1}{4}\cos(\omega t) + \tfrac{1}{2}\cos(3\omega t) - \tfrac{1}{4}\cos(5\omega t) \tag{A12}$$

$$\sin(\omega t)\sin(3\omega t)\cos(3\omega t) = \tfrac{1}{4}\cos(5\omega t) - \tfrac{1}{4}\cos(7\omega t) \tag{A13}$$

$$\sin(\omega t)\cos^2(3\omega t) = \tfrac{1}{2}\sin(\omega t) - \tfrac{1}{4}\sin(5\omega t) + \tfrac{1}{4}\sin(7\omega t) \tag{A14}$$

$$\sin(3\omega t)\cos^2(3\omega t) = \tfrac{1}{4}\sin(3\omega t) + \tfrac{1}{4}\sin(9\omega t) \tag{A15}$$

$$\sin(3\omega t)^2\cos(3\omega t) = \tfrac{1}{4}\cos(3\omega t) - \tfrac{1}{4}\cos(9\omega t) \tag{A16}$$

$$\sin^3(\omega t) = \tfrac{3}{4}\sin(\omega t) - \tfrac{1}{4}\sin(3\omega t) \tag{A17}$$

$$\sin^2(\omega t)\sin(3\omega t) = -\tfrac{1}{4}\sin(\omega t) + \tfrac{1}{2}\sin(3\omega t) - \tfrac{1}{4}\sin(5\omega t) \tag{A18}$$

$$\sin(\omega t)\sin^2(3\omega t) = \tfrac{1}{2}\sin(\omega t) + \tfrac{1}{4}\sin(5\omega t) - \tfrac{1}{4}\sin(7\omega t) \tag{A19}$$

$$\sin^3(3\omega t) = \tfrac{3}{4}\sin(3\omega t) - \tfrac{1}{4}\sin(9\omega t) \tag{A20}$$